Derivation of wave functions and matrix elements of the residual interaction in ^{208}Pb from experimental data

M. Rejmund,* M. Schramm,† and K. H. Maier‡
Hahn-Meitner-Institut Berlin, Postfach 390128, D-14091 Berlin, Germany
(Received 22 December 1998)

Shell-model wave functions for many states of ^{208}Pb have been derived in a strictly empirical way from measured spectroscopic factors and branching ratios of γ transitions. It was assumed that the lowest n states of a given I^π can be described by an orthonormal superposition of the n lowest one-particle one-hole configurations for this I^π. The often highly redundant data are well reproduced. The matrix elements of the residual interaction were calculated from the wave functions by inverting the Schrödinger equation. The diagonal matrix elements show clear and reasonable trends. The set of empirical $M1$ and $E2$ single particle matrix elements that has been used is presented. [S0556-2813(99)04905-5]

PACS number(s): 21.30.Fe, 21.60.Cs, 23.20.Lv, 27.80.+w

I. INTRODUCTION

The shell model describes many properties of doubly magic ^{208}Pb and neighboring nuclei very well. Also many properties of these nuclei can be measured as ^{208}Pb itself and two of its neighbors are stable and can be used as targets. For comparison, ^{100,132}Sn and also ^{56}Ni are less accessible for experiments, and ^{16}O and ^{40}Ca are light nuclei. In this article we deduce wave functions of many levels below 5 MeV excitation energy in ^{208}Pb, making use of the fact that the level scheme is practically complete below 5 MeV and many properties of these states are known. The wave functions are restricted, to include only the lowest one particle one hole excitations; the results justify this simplification. In a next step then the matrix elements of the residual interaction are calculated from the deduced wave functions and measured level energies by inverting the Schrödinger equation. Around 100 empirical matrix elements are derived in this way, they might be used to check and adjust theoretical interactions. A similar approach to deduce the interaction from measured data has already been used by Heusler and von Brentano [1]. Unfortunately they were misled by some wrong spin assignments at the time.

Several interactions have been rather successfully applied. True, Ma, and Pinkston used a phenomenological singlet even plus quadrupole force to calculate the negative parity one particle one hole levels of ^{208}Pb [2]. Kuo and Herling [3] have deduced a realistic interaction from the Hamada-Johnston potential between free nucleons following the method of Kuo and Brown [4]. They calculated wave functions for the two particle and two hole nuclei around ^{208}Pb, but unfortunately no results on ^{208}Pb itself have been published. This realistic interaction has been found to explain many data quite well, in particular after some small adjustments [5].

The measured energies of the states with the appropriate I^π in the nuclei with one nucleon more or less than ^{208}Pb are taken as the single particle energies in the mentioned theoretical calculations and the following treatment. Figure 1 shows the single particle orbitals with these energies. Parts of this work have been already presented at conferences [6,7] and in a Ph.D. and diploma thesis [8,9].

II. DERIVATION OF THE WAVE FUNCTIONS

A. The experimental data

The experimental data of Schramm *et al.* [10] are the basis of this analysis. They include sets of spectroscopic factors for the proton pick up reaction ^{209}Bi$(t,\alpha)^{208}$Pb and the neutron transfer reaction ^{207}Pb$(d,p)^{208}$Pb and many γ-branching ratios. Table V of this reference gives the experimental level scheme of ^{208}Pb, that is used here. More recent γ spectroscopy with the ^{208}Pb$(n,n')^{208}$Pb reaction by

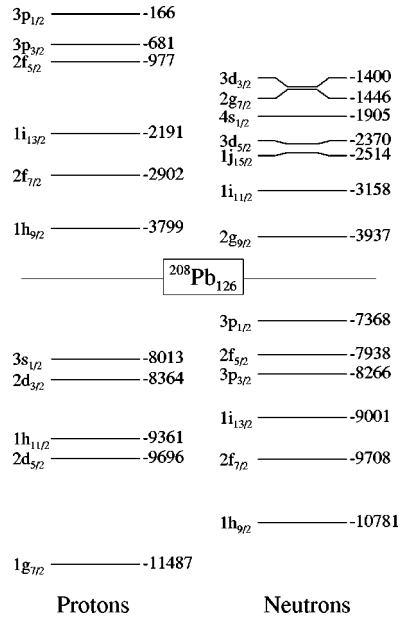

FIG. 1. Single particle orbitals around ^{208}Pb and their energies relative to ^{208}Pb.

*Present address: Centre de Spectrometrie Nucleaire et de Spectrometrie de Masse, bat. 104, 91405 Orsay Campus, France.
†Present address: Wesendonkstrasse 31, D-81925 München, Germany.
‡Electronic mail: Maier@hmi.de

Yeh *et al.* [11,12] has essentially confirmed the results of Schramm *et al.* [10]. Also a new, very high resolution study of inelastic scattering and transfer reactions with the Q3D spectrometer at the Munich tandem [13] agrees nearly always with the used data [10]. Only their results from the investigation of the ^{207}Pb$(d,p)^{208}$Pb reaction with polarized deuterons show that there is some mixing between the $\nu 3d_{3/2}3p_{1/2}^{-1}$ and $\nu 3d_{5/2}3p_{1/2}^{-1}$ configurations, that had been excluded in the evaluation of spectroscopic factors by Schramm *et al.* [10]. This and a few new levels from Yeh *et al.* and Valnion *et al.* [11,13] have not been included in the present analysis.

B. General procedure

A qualitative inspection of the experimental data shows already that the wave functions of the excited states of ^{208}Pb are well described by a superposition of few single particle–single hole configurations. The energies of the real states lie close to the unperturbed particle-hole energies. Therefore the residual interaction is weak, and two particle–two hole excitations are unimportant; they are about 3 MeV higher in energy, while the mixing matrix elements are of the order of 100 keV. Therefore we try in the following to reproduce the measured properties of the real levels by simple wave functions. The wave functions ψ_i of the n lowest lying states of a given spin and parity I^π are described as

$$\psi_i = a_{i1}\phi_1 + a_{i2}\phi_2 + \cdots + a_{in}\phi_n \quad \text{with} \quad i = 1 \ldots n.$$

The ϕ_i are the n particle-hole configurations that can couple to the given I^π and are lowest in energy. The energies of the proton configurations are lowered by 300 keV to account for the Coulomb pairing energy. This means that the n^2 amplitudes a_{ik} have to be determined. But, taking the model seriously, the wave functions are orthonormal, which gives $n(n+1)/2$ conditions and reduces the number of free parameters to $n(n-1)/2$. The number of considered levels n is arbitrarily determined by the availability of experimental data. Mixing with higher states should be considered. In some cases, as for $10+$ states, the next configuration is much higher in energy and can be neglected. In general, the wave function of the highest state included in the analysis serves mainly to fulfill the orthonormality requirement for the lower states and is not very meaningful.

The number of $M1$ transitions that can occur between the n states of a given I^π is $n(n-1)/2$. This would already match the number of free parameters. But only branching ratios have been measured, no lifetimes, and their number is $n(n-3)/2+1$. This leaves $n-1$ free parameters. If configurations with either a hole in the $\nu 3p_{1/2}$ orbital or a particle in the $\pi 1h_{9/2}$ orbital are involved the measured spectroscopic factors give directly the n a_{ik}^2, and the system is already overdetermined. More information is available from other multipolarities and the transitions to and from levels with different I^π. But some amplitudes might be little sensitive to any measured data and therefore poorly determined, while others are very well determined. The examples given below will demonstrate this in some detail.

The wave functions have been determined by trial and error. Usually the main component was clear from the spectroscopic factors; otherwise it could be guessed from the energy of the state. Spectroscopic factors often also fixed some smaller amplitudes right away. This determined the first trial wave functions, that contained no other admixtures. $M1$ and $E2$ transition rates were then calculated for the trial wave functions. These calculations gave also the individual contributions to the transition rates from each involved configuration and the derivatives of the transition strengths relative to the amplitudes of the wave function. This allowed to judge, which amplitudes had to be modified in order to achieve better agreement between measured and calculated branching ratios. The set of wave functions for a given I^π was also orthonormalized repeatedly using the Schmidt procedure. The whole process was then repeated until either agreement with experiment had been reached or we could not make progress anymore. The optimization is fairly complicated; the requirement of orthonormalized wave functions connects all amplitudes for a given I^π, and states of different spin have also to be treated simultaneously, if there are connecting γ transitions.

The calculation of the γ-transition rates is straightforward. The transition matrix element between the particle-hole configurations is calculated from the single particle and hole elements by angular momentum coupling (see, e.g., Ref. [14]). The total transition element between two states results then from adding the contributions of the various configurations in the initial and final state. This coherent superposition is often very sensitive to small amplitudes and of course to the signs of the amplitudes. The single particle $M1$ and $E2$ matrix elements, that have been used are presented in the Appendix. These are effective matrix elements appropriate for our restriction to one particle–one hole configurations. They account for the particular core excitations that lead to the effective quadrupole charge and the deviations of the magnetic moments from the Schmidt values. By far the most γ transitions are of M1 multipolarity. $E2$ transitions can compete in rare cases only, and $E1$, $M2$, and $E3$ transitions are very scarce.

Approximate errors of the amplitudes in the wave functions have also been determined [9]. This is still more difficult than the derivation of the amplitudes themselves. We looked for those pieces of the experimental data, that are mainly sensitive to just one amplitude and little influenced by others and assigned the errors from them. A proper treatment would require an unwieldy error matrix. Meaningful errors could be assigned to some amplitudes and are stated in Table I and in part discussed for individual levels below.

The collective 3^- state at 2.615 MeV is too complicated to be treated in this way. We took the 25 largest components of a wave function calculated by Warburton [15]. The γ transitions to this level are mostly not well reproduced and have not been used in the analysis. Admixtures of the collective octupole to the particle-hole configurations have not been taken into account explicitly. Instead the single particle orbitals that we use are not really pure but include admixtures of this type. For instance the $\nu 1j_{15/2}$ orbital contains a $\nu 2g_{9/2}\times 3^-$ admixture.

The wave functions derived in this way are presented in Table I. This table contains also the square roots of the measured spectroscopic factors [10] in *italic* for comparison; they should equal the absolute values of the deduced ampli-

TABLE I. Empirical wave functions in ^{208}Pb. Below the measured level energies the amplitudes of the indicated particle-hole configurations are presented. Errors of the amplitudes are given, if they could be determined. Absence of an error means usually that this amplitude is not well determined. Square roots of spectroscopic factors are shown below the corresponding amplitudes in *italic*. See also the text.

						0^- states						
Energy (keV)	5280.3		5599.4									
Configuration						Amplitude						
$\nu 4s_{1/2}3p^{-1}_{1/2}$	0.93	(13)	0.37	(23)								
	0.93		*0.37*									
$\nu 3d_{5/2}2f^{-1}_{5/2}$	−0.37	(25)	0.93	(15)								
						1^- states						
Energy (keV)	4841.4		5292.0		5512.1							
Configuration						Amplitude						
$\nu 4s_{1/2}3p^{-1}_{1/2}$	0.03	(3)	0.91	(10)	0.40							
	0.10		*0.96*		*0.25*							
$\nu 3d_{5/2}2f^{-1}_{5/2}$	0.24		0.38		−0.89							
$\nu 2g_{9/2}2f^{-1}_{7/2}$	0.96		−0.13		0.20							
						2^- states						
Energy (keV)	4229.6		5037.5		5127.4							
Configuration						Amplitude						
$\nu 2g_{9/2}2f^{-1}_{5/2}$	0.94		0.33		−0.02							
$\nu 3d_{5/2}3p^{-1}_{1/2}$	0.28		−0.76		0.57							
	0.24		*0.80*		*0.55*							
$\pi 2f_{7/2}2d^{-1}_{3/2}$	−0.17		0.54		0.81							
						3^- states						
Energy (keV)	2614.5		4051.2		4254.9		4698.4		4937.6			
Configuration						Amplitude						
$\nu 2g_{9/2}2f^{-1}_{5/2}$			−0.95		−0.20		0.00		0.00			
$\pi 1h_{9/2}2d^{-1}_{3/2}$	−0.35		−0.16		0.70		0.42		0.00			
	0.39		*0.18*		*0.76*		*0.49*					
$\nu 2g_{9/2}3p^{-1}_{3/2}$			−0.30		−0.70		0.53		0.00			
$\nu 1i_{11/2}2f^{-1}_{5/2}$			0.00		0.00		−0.50		0.45			
$\pi 2f_{7/2}3s^{-1}_{1/2}$			0.00		0.00		−0.25		−0.90			
						4^- states						
Energy (keV)	3475.1		3946.6		3995.6		4262.0		4358.8			
Configuration						Amplitude						
$\nu 2g_{9/2}3p^{-1}_{1/2}$	0.97	(6)	−0.10	(5)	0.10	(4)	0.10	(6)	−0.20	(10)		
	0.99		*0.05*		*0.11*		*0.05*		*0.10*			
$\pi 1h_{9/2}3s^{-1}_{1/2}$	0.10	(4)	0.92	(6)	−0.21	(4)	−0.30	(4)	−0.15	(3)		
	0.07		*0.92*		*0.22*		*0.27*		*0.16*			
$\nu 2g_{9/2}2f^{-1}_{5/2}$	−0.14	(10)	0.20	(7)	0.95	(10)	0.03		−0.18			
$\pi 1h_{9/2}2d^{-1}_{3/2}$	0.10	(10)	0.34	(5)	0.00	(10)	0.79	(6)	0.50	(5)		
	0.00		*0.38*		*0.00*		*0.76*		*0.51*			
$\nu 2g_{9/2}3p^{-1}_{3/2}$	0.20		0.00		0.20	(15)	−0.52		0.81			
						5^- states						
Energy (keV)	3197.7		3708.5		3961.1		4125.4		4180.2		4296.7	
Configuration						Amplitude						
$\nu 2g_{9/2}3p^{-1}_{1/2}$	−0.95	(10)	0.26	(5)	0.04	(3)	0.04	(4)	0.08	(8)	−0.07	(5)
	0.89		*0.43*		*0.00*		*0.11*		*0.00*		*0.05*	
$\pi 1h_{9/2}3s^{-1}_{1/2}$	0.25	(2)	0.61	(3)	0.62	(5)	0.23	(4)	0.26	(15)	−0.20	(9)
	0.26		*0.59*		*0.67*		*0.19*		*0.11*		*0.29*	
$\nu 2g_{9/2}2f^{-1}_{5/2}$	−0.15	(2)	−0.63	(6)	0.72	(10)	0.13	(7)	−0.11	(9)	0.11	
$\nu 1i_{11/2}3p^{-1}_{1/2}$	0.00	(3)	−0.26	(2)	0.04		−0.56	(10)	0.56		−0.54	
	0.00		*0.00*		*0.00*		*0.71*		*0.71*		*0.00*	
$\pi 1h_{9/2}2d^{-1}_{3/2}$	0.00	(5)	0.26	(2)	0.26	(4)	−0.76	(6)	−0.18	(2)	0.50	(3)
	0.00		*0.28*		*0.29*		*0.70*		*0.18*		*0.48*	
$\nu 2g_{9/2}3p^{-1}_{3/2}$	0.00	(6)	0.08	(18)	0.08	(6)	−0.17	(10)	−0.74	(15)	−0.62	

TABLE I. (*Continued*).

					6^- states					
Energy (keV)	3919.9		4206.2		4383.2		4480.7		4761.8	
Configuration						Amplitude				
$\nu 2g_{9/2}2f_{5/2}^{-1}$	0.99	(10)	−0.02	(2)	−0.09	(10)	0.02		0.00	
$\nu 1i_{11/2}3p_{1/2}^{-1}$	0.00	(10)	0.97	(3)	−0.18	(2)	0.12	(10)	0.02	(10)
	0.00		*0.95*		*0.16*		*0.00*		*0.00*	
$\pi 1h_{9/2}2d_{3/2}^{-1}$	0.10	(4)	0.21	(2)	0.93	(3)	−0.27	(9)	−0.05	(10)
	0.00		*0.21*		*0.91*		*0.36*		*0.00*	
$\nu 2g_{9/2}3p_{3/2}^{-1}$	0.03	(2)	−0.07	(2)	0.29	(5)	0.93		0.19	
$\nu 1i_{11/2}2f_{5/2}^{-1}$	0.00		0.00		0.00		−0.20		0.97	
					6^+ states					
Energy (keV)	4423.6		5213.0							
Configuration						Amplitude				
$\nu 2g_{9/2}1i_{13/2}^{-1}$	0.91	(10)	−0.42	(10)						
$\pi 1h_{9/2}1h_{11/2}^{-1}$	0.42	(4)	0.91	(5)						
	0.48		*0.88*							
					7^- states					
Energy (keV)	4037.5		4680.3		5085.5		5543.0		5695.1	
Configuration						Amplitude				
$\nu 2g_{9/2}2f_{5/2}^{-1}$	0.99	(10)	0.00		0.00		−0.03	(7)	−0.09	
$\nu 1i_{11/2}2f_{5/2}^{-1}$	0.00		1.00	(15)	0.00		0.00		0.00	
$\nu 1i_{11/2}3p_{3/2}^{-1}$	0.00		0.00		0.95	(10)	−0.29	(9)	0.09	
$\pi 1h_{9/2}2d_{5/2}^{-1}$	0.03	(10)	0.00	(10)	0.31	(2)	0.90	(5)	-0.28	(3)
	0.00		*0.00*		*0.27*		*0.91*		*0.32*	
$\nu 2g_{9/2}2f_{7/2}^{-1}$	0.10	(5)	0.00		0.00		0.30	(4)	0.94	(16)
					7^+ states					
Energy (keV)	4867.8		5195.3							
Configuration						Amplitude				
$\nu 1j_{15/2}3p_{1/2}^{-1}$	0.92		−0.30							
	1.00		*0.00*							
$\nu 2g_{9/2}1i_{13/2}^{-1}$	0.40		0.50							
$\pi 1h_{9/2}1h_{11/2}^{-1}$	0.10		0.85							
	0.00		*1.00*							
					8^+ states					
Energy (keV)	4610.8		4860.8		5093.1		5339.5		5826.2	
Configuration						Amplitude				
$\nu 1j_{15/2}3p_{1/2}^{-1}$	−0.78	(5)	0.62	(5)	0.00		0.00		0.00	
	0.81		*0.59*		*0.00*		*0.00*		*0.00*	
$\nu 2g_{9/2}1i_{13/2}^{-1}$	0.44	(10)	0.55	(30)	0.60	(17)	0.35	(18)	0.00	
$\pi 1h_{9/2}1h_{11/2}^{-1}$	−0.42	(3)	−0.53	(7)	0.59	(10)	0.34	(20)	0.25	(8)
	0.40		*0.45*		*0.50*		*0.56*		*0.26*	
$\nu 1j_{15/2}2f_{5/2}^{-1}$	0.00		0.00		−0.50		0.86		0.00	
$\nu 1j_{15/2}3p_{3/2}^{-1}$	0.11		0.14		−0.15		−0.09		0.96	(36)
					9^+ states					
Energy (keV)	5010.5		5162.1							
Configuration						Amplitude				
$\nu 2g_{9/2}1i_{13/2}^{-1}$	0.98	(15)	−0.20	(14)						
$\pi 1h_{9/2}1h_{11/2}^{-1}$	0.20	(3)	0.98	(5)						
	0.17		*0.98*							
					10^+ states					
Energy (keV)	4895.3		5069.4		5536.6		5928.0			
Configuration						Amplitude				
$\nu 2g_{9/2}1i_{13/2}^{-1}$	0.79	(17)	0.38	(17)	0.46	(10)	−0.13	(20)		
$\pi 1h_{9/2}1h_{11/2}^{-1}$	−0.57	(5)	0.66	(5)	0.36	(5)	−0.33	(5)		
	0.58		*0.58*		*0.41*		*0.40*			
$\nu 1j_{15/2}2f_{5/2}^{-1}$	−0.19	(8)	−0.51		0.81		0.21			
$\nu 1i_{11/2}1i_{13/2}^{-1}$	−0.05	(8)	0.41	(25)	0.01		0.91			

tudes. As the levels with $I \geqslant 11$ have pure wave functions they are not listed in Table I. Table II compares the measured γ-branching ratios with those calculated from the wave functions. A discussion follows in the next subsections.

C. The 0^-, 1^-, 2^-, and 3^- states

The two 0^- states are well separated in energy from the next state of this spin. The one free mixing parameter is determined by the spectroscopic factors for the configuration $\nu 4s_{1/2}3p_{1/2}^{-1}$. This mixing reproduces also their γ decay to the first 1^- and 2^- state quantitatively. The three lowest 1^- and 2^- levels have been considered because they have been populated in (d,p). The next level is close in both cases, and therefore the wave functions of the third state are wrong. The 1^- states decay by $E1$ to the ground state; this gives no information for the present analysis. Also the decay of the 2^- levels to the collective 3^- state contains little information. The relative branching from the second 2^- to the 4^- and 2^- levels is well reproduced, while the decays to the 3^- levels do not fit well due to the problems in describing the 3^- states.

The wave functions of the 3^- states have only been treated superficially. The collective state is of too complicated structure and the collectivity of the first 3^- state prevents also a strict orthogonalization for all other levels. Nevertheless the wave functions are approximately orthonormal and reproduce the spectroscopic factors of the proton pick up and γ decays reasonably. But the $\nu 3d_{5/2}3p_{1/2}^{-1}$ configuration is not included in the analysis, although it is populated in the (d,p) reaction.

D. The 4^- and 5^- states

Three sets of spectroscopic factors have been measured for the 4^- states and 4 for 5^-. But the distinction between $3s_{1/2}$ and $2d_{3/2}$ proton pickup and $2g_{9/2}$ and $1i_{11/2}$ neutron transfer relies on the angular distribution of the particles. A redistribution of some strength from $2g_{9/2}$ to $1i_{11/2}$ for the 3708.5 keV 5^- level reproduces the γ decays much better. The γ branching ratios are well but not perfectly reproduced. Often very small changes of the amplitudes ($\sim$0.03) influence the γ decay strongly. Orthonormalizing the wave functions gives changes of this magnitude that can destroy the previously achieved agreement with experiment. Small admixtures are especially important if the γ decay for the main components is slow or completely forbidden; the calculated half lives of Table II indicate this. Likely the data could be better fitted with a more powerful mathematical procedure. But higher lying configurations might also have to be considered; this is definitely the case for the highest states. There are only 16 free parameters for the combined 4^- and 5^- states. They are 3 times overdetermined. The agreement between measured and calculated properties is remarkable.

The neutron components of the lowest 4^- state have been determined from the differential cross section of (p,p') through the $2g_{9/2}$ analog resonance by Bondorf *et al.* [16]. They derived $a(\nu 2g_{9/2}3p_{1/2}^{-1}) = 0.94(2)$, $a(\nu 2g_{9/2}2f_{5/2}^{-1}) = 0.07(16)$, and $a(\nu 2g_{9/2}3p_{3/2}^{-1}) = -0.24(3)$. Except for the sign of the two small components this agrees very well with the present result. Richard *et al.* [17] derived from the same (p,p') data for the 3.708 MeV 5^- state: $a(\nu 2g_{9/2}3p_{1/2}^{-1}) = 0.41(2)$, $a(\nu 2g_{9/2}2f_{5/2}^{-1}) = -0.76(12)$, and $a(\nu 2g_{9/2}3p_{3/2}^{-1}) = 0.10(18)$. The first amplitude is taken from the spectroscopic factor of the (d,p) reaction. Our amplitude is smaller, because the γ-decay favors to ascribe part of the (d,p) strength to $1i_{11/2}$ transfer; otherwise the agreement is perfect.

E. The 6^- and 7^- states

The lowest four 6^- states are definitely identified. The 4761 keV level is identified as the fifth, because it decays to the 3198 keV 5^- level, and the only state expected by the shell model, that fits this energy and decay is 6^-. Therefore these 5 states are described by a superposition of the 5 lowest configurations that give $I^\pi = 6^-$, namely $\nu 2g_{9/2}2f_{5/2}^{-1}$, $\nu 1i_{11/2}3p_{1/2}^{-1}$, $\pi 1h_{9/2}2d_{3/2}^{-1}$, $\nu 2g_{9/2}3p_{3/2}^{-1}$, $\nu 1i_{11/2}2f_{5/2}^{-1}$. The configurations $\nu 1i_{11/2}3p_{1/2}^{-1}$ and $\pi 1h_{9/2}2d_{3/2}^{-1}$ are populated in the transfer reactions and therefore 10 spectroscopic factors are known.

The 6_1^- state is discussed as an example in the following. The dominant component of the 6_1^- state is $\nu 2g_{9/2}2f_{5/2}^{-1}$. The amplitudes of the $\nu 1i_{11/2}3p_{1/2}^{-1}$ and $\pi 1h_{9/2}2d_{3/2}^{-1}$, vanish according to the spectroscopic factors. The absence of a γ transition from the 7_3^- and the weak transition from 7_4^- set also limits on these amplitudes. The dominant configurations of these 7^- states, namely $\nu 1i_{11/2}3p_{3/2}^{-1}$ and $\pi 1h_{9/2}2d_{5/2}^{-1}$, would otherwise lead to strong transitions to 6_1^-. Likewise the adopted amplitude $a(6_1^-, \pi 1h_{9/2}2d_{3/2}^{-1}) = 0.1$ gives already a somewhat too large branching from the predominantly $\pi 1h_{9/2}2d_{3/2}^{-1}$ 6_3^- to 6_1^-. All these transitions proceed from the main components of the decaying states, that are well known, with strong transition matrix elements. Therefore they determine the amplitudes for the 6_1^- with little uncertainty from other possible contributions.

The small amplitude $a(6_1^-, \nu 2g_{9/2}3p_{3/2}^{-1}) = 0.03$ is well determined by the branching ratio of the decay to 5_1^- and 5_2^-, because this configuration is connected by a strong $M1$ matrix element to the main configuration $\nu 2g_{9/2}3p_{1/2}^{-1}$ of the first 5^- state. Table III shows the destructive interference in the $M1$ decay to 5_1^-, that is needed to reproduce the branching ratio. The 6_1^- to 5_1^- transition contains also an $E2$ component (see Table III). Also for this a destructive interference between the two main amplitudes $\nu 2g_{9/2}2f_{5/2}^{-1},6^-$ to $\nu 2g_{9/2}2f_{5/2}^{-1},5^-$ and $\nu 2g_{9/2}2f_{5/2}^{-1},6^-$ to $\nu 2g_{9/2}3p_{1/2}^{-1},5^-$ is required. As both components proceed from the same configuration in the 6^- level, its sign drops out and the relative sign of the two configurations of the 5^- state is fixed. The $M1$ component determines now the relative signs of the $\nu 2g_{9/2}2f_{5/2}^{-1}$ and $\nu 2g_{9/2}3p_{3/2}^{-1}$ configurations in the 6^- state. This is an example for the determination of signs.

The partial derivatives of the branch from 6_1^- to 5_1^- relative to all involved amplitudes are shown in Fig. 2. From plots like this it is evident, which amplitudes matter for the particular measured branching ratio and are therefore well determined. In the presented case, the $\nu 2g_{9/2}3p_{3/2}^{-1}$ configuration of the 6^- state and the $\nu 2g_{9/2}2f_{5/2}^{-1}$ configuration of the 5_1^- state are dominant. The second mentioned amplitude cannot vary much, as otherwise for instance the weak

TABLE II. γ-branching ratios calculated from the empirical wave functions in comparison with experiment. The columns show energy and spin of the decaying and populated state, multipolarity, γ energy, the theoretical branching ratio as calculated from the wave functions, and the measured branching ratio with its error. The measured branching ratios for mixed $M1/E2$ transitions give the combined intensity and are to be compared with the sum of the theoretical branchings. Experimental decays by other than $M1$ or $E2$ transitions are not included; therefore the summed strength of the branches might be $\leqslant$100%. All branches are included, for which the theoretical strength is $\geqslant$1% or a transition has been measured. The total theoretical halflife for each decaying state is also given.

Init.		Final		Λ	E_γ	b_{th}	b_{exp}	Err.
5280.5	0^-	4229.5	2^-	$E2$	1051.0	79.1	78.4	2.2
		4841.7	1^-	$M1$	438.8	20.8	21.6	1.0
$T_{1/2}=0.14E-10s$								
5598.0	0^-	4229.5	2^-	$E2$	1368.5	59.5	66.9	5.8
		4841.7	1^-	$M1$	756.3	36.9	33.1	3.3
		5037.4	2^-	$E2$	560.6	1.9		
		5512.5	1^-	$M1$	85.5	1.3		
$T_{1/2}=0.21E-11s$								
4229.5	2^-	2614.6	3^-	$M1$	1614.9	98.6	88.6	8.9
		4051.3	3^-	$M1$	178.2	1.3		
$T_{1/2}=0.33E-12s$								
5037.4	2^-	2614.6	3^-	$M1$	2422.8	42.4	85.4	5.7
		2614.6	3^-	$E2$	2422.8	1.9		
		3475.1	4^-	$E2$	1562.3	28.5	6.4	0.4
		4051.3	3^-	$M1$	986.1	10.1	3.3	0.2
		4229.5	2^-	$M1$	807.9	15.0	3.8	0.4
		4698.5	3^-	$M1$	338.9	1.2		
$T_{1/2}=0.12E-12s$								
5127.3	2^-	2614.6	3^-	$M1$	2512.8	33.5	87.6	3.1
		3475.1	4^-	$E2$	1652.2	14.9	5.8	0.7
		4229.5	2^-	$M1$	897.8	49.8		
$T_{1/2}=0.13E-12s$								
4051.3	3^-	2614.6	3^-	$M1$	1436.7	95.6	84.5	4.7
		3475.1	4^-	$M1$	576.1	3.4	15.5	1.5
$T_{1/2}=0.12E-12s$								
4254.4	3^-	2614.6	3^-	$M1$	1639.9	91.8	75.0	9.6
		3475.1	4^-	$M1$	779.3	7.8	25.0	4.8
$T_{1/2}=0.39E-13s$								
4698.5	3^-	2614.6	3^-	$M1$	2083.9	5.9	11.2	1.2
		3197.7	5^-	$E2$	1500.7	24.7	17.7	1.1
		3475.1	4^-	$M1$	1223.4	48.5	40.9	2.0
		3946.6	4^-	$M1$	751.8	3.6		
		3995.9	4^-	$M1$	702.5	0.2	1.7	0.2
		4051.3	3^-	$M1$	647.2	5.1	1.7	0.3
		4229.5	2^-	$M1$	469.0	0.1	4.1	0.4
		4254.4	3^-	$M1$	444.1	10.0	16.8	0.8
		4262.0	4^-	$M1$	436.5	0.1	3.6	0.3
$T_{1/2}=0.13E-12s$								
4938.5	3^-	2614.6	3^-	$M1$	2323.9	98.7	93.6	24.6
		2614.6	3^-	$E2$	2323.9	1.0		
$T_{1/2}=0.11E-13s$								
5317.0	3^+	4324.0	4^+	$M1$	993.0	95.1	79.9	8.0
		4324.0	4^+	$E2$	993.0	4.0		
$T_{1/2}=0.48E-12s$								
3475.1	4^-	2614.6	3^-	$M1$	860.6	36.4	65.3	2.1
		3197.7	5^-	$M1$	277.4	63.5	34.7	1.3
$T_{1/2}=0.43E-11s$								
3946.6	4^-	2614.6	3^-	$M1$	1332.1	34.4		
		3197.7	5^-	$M1$	748.9	47.8	66.0	4.6
		3475.1	4^-	$M1$	471.5	12.5	17.4	1.2
		3708.4	5^-	$M1$	238.2	5.1	16.7	1.2

TABLE II. (*Continued*).

Init.		Final		Λ	E_γ	b_{th}	b_{exp}	Err.
$T_{1/2}=0.59E-12s$								
3995.9	4^-	2614.6	3^-	$M1$	1381.4	58.4	81.9	20.2
		3197.7	5^-	$M1$	798.2	33.9	18.1	4.3
		3197.7	5^-	$E2$	798.2	1.2		
		3708.4	5^-	$M1$	287.5	5.5		
$T_{1/2}=0.39E-12s$								
4262.0	4^-	2614.6	3^-	$M1$	1647.4	1.1	48.5	3.9
		2614.6	3^-	$E2$	1647.4	1.4		
		3197.7	5^-	$M1$	1064.2	0.0	2.1	0.3
		3475.1	4^-	$M1$	786.9	34.1	27.0	2.2
		3708.4	5^-	$M1$	553.6	57.7	22.4	1.8
		3961.1	5^-	$M1$	300.9	3.7		
$T_{1/2}=0.95E-12s$								
4358.8	4^-	2614.6	3^-	$M1$	1744.3	29.4	11.7	1.7
		2614.6	3^-	$E2$	1744.3	1.3		
		3197.7	5^-	$M1$	1161.1	11.9	23.8	3.6
		3197.7	5^-	$E2$	1161.1	1.1		
		3475.1	4^-	$M1$	883.7	53.0	61.5	5.5
		3961.1	5^-	$M1$	397.7	1.9		
		3995.9	4^-	$M1$	362.9	0.5	1.7	0.4
		4180.4	5^-	$M1$	178.4	0.1	1.3	0.6
$T_{1/2}=0.10E-12s$								
3197.7	5^-	2614.6	3^-	$E2$	583.2	100.0	100.0	3.1
$T_{1/2}=0.58E-09s$								
3708.4	5^-	2614.6	3^-	$E2$	1093.9	0.4	3.0	0.8
		3197.7	5^-	$M1$	510.7	97.5	95.2	4.8
		3475.1	4^-	$M1$	233.3	2.1	1.8	0.6
$T_{1/2}=0.11E-11s$								
3961.1	5^-	3197.7	5^-	$M1$	763.4	74.7	68.6	4.8
		3475.1	4^-	$M1$	486.0	0.1	1.6	0.6
		3708.4	5^-	$M1$	252.7	24.3	29.8	2.1
$T_{1/2}=0.24E-12s$								
4125.5	5^-	2614.6	3^-	$E2$	1510.9	5.4		
		3197.7	5^-	$M1$	927.7	83.9	77.1	9.3
		3475.1	4^-	$M1$	650.3	9.3	14.7	3.0
		3708.4	5^-	$M1$	417.0	0.8	3.7	0.8
		3946.6	4^-	$M1$	178.8	0.2	0.7	0.2
		3961.1	5^-	$M1$	164.3	0.0	3.7	0.5
$T_{1/2}=0.43E-12s$								
4180.4	5^-	2614.6	3^-	$E2$	1565.9	1.2		
		3197.7	5^-	$M1$	982.7	82.4	83.8	8.5
		3475.1	4^-	$M1$	705.3	11.4	16.2	4.2
		3708.4	5^-	$M1$	472.0	4.0		
$T_{1/2}=0.87E-13s$								
4296.7	5^-	3197.7	5^-	$M1$	1098.9	19.3	5.2	1.6
		3475.1	4^-	$M1$	821.6	59.3	33.3	3.4
		3708.4	5^-	$M1$	588.2	1.2	58.4	5.9
		3919.9	6^-	$M1$	376.8	1.8		
		3946.6	4^-	$M1$	350.0	2.5		
		3961.1	5^-	$M1$	335.6	2.2		
		4125.5	5^-	$M1$	171.2	9.9	3.1	0.8
		4180.4	5^-	$M1$	116.3	1.8		
$T_{1/2}=0.57E-12s$								
5193.3	5^+	4324.0	4^+	$M1$	869.3	50.0	45.0	4.5
		4324.0	4^+	$E2$	869.3	2.7		
		4423.5	6^+	$M1$	769.8	44.5	45.2	12.6
		4423.5	6^+	$E2$	769.8	2.8		

TABLE II. (*Continued*).

Init.		Final		Λ	E_γ	b_{th}	b_{exp}	Err.
$T_{1/2}=0.51E-12s$								
3919.9	6^-	3197.7	5^-	$M1$	722.2	48.6	55.2	6.2
		3197.7	5^-	$E2$	722.2	13.2		
		3708.4	5^-	$M1$	211.5	37.3	44.8	4.1
$T_{1/2}=0.14E-10s$								
4206.3	6^-	3197.7	5^-	$M1$	1008.6	79.4	82.2	5.7
		3197.7	5^-	$E2$	1008.6	4.0		
		3708.4	5^-	$M1$	497.9	15.0	17.8	2.3
		3919.9	6^-	$M1$	286.4	1.1		
$T_{1/2}=0.56E-11s$								
4383.3	6^-	3197.7	5^-	$M1$	1185.5	88.3	93.8	17.8
		3197.7	5^-	$E2$	1185.5	1.1		
		3919.9	6^-	$M1$	463.4	7.9	4.8	0.7
		4125.5	5^-	$M1$	257.8	0.6	0.6	0.2
		4206.3	6^-	$M1$	176.9	0.7	0.8	0.2
$T_{1/2}=0.33E-12s$								
4480.8	6^-	3197.7	5^-	$M1$	1283.0	94.2	94.0	8.5
		3708.4	5^-	$M1$	772.3	4.1	6.0	2.5
$T_{1/2}=0.60E-13s$								
4761.8	6^-	3197.7	5^-	$M1$	1564.1	85.0	100.0	30.0
		3961.1	5^-	$M1$	800.7	3.8		
		4383.3	6^-	$M1$	378.5	4.0		
		4480.8	6^-	$M1$	281.0	2.3		
$T_{1/2}=0.53E-12s$								
4037.6	7^-	3197.7	5^-	$E2$	839.8	92.4	88.4	13.7
		3919.9	6^-	$M1$	117.7	7.5	11.6	4.2
$T_{1/2}=0.19E-10s$								
4680.2	7^-	3708.4	5^-	$E2$	971.8	3.6		
		3919.9	6^-	$M1$	760.3	88.5	100.0	30.0
		4037.6	7^-	$M1$	642.6	3.7		
		4206.3	6^-	$E2$	473.9	1.8		
$T_{1/2}=0.85E-11s$								
5085.5	7^-	3197.7	5^-	$E2$	1887.8	1.0		
		3708.4	5^-	$E2$	1377.1	2.3		
		4206.3	6^-	$M1$	879.2	77.3	88.8	9.7
		4383.3	6^-	$M1$	702.3	11.2	11.2	3.7
		4480.8	6^-	$M1$	604.7	5.4		
$T_{1/2}=0.15E-12s$								
5543.0	7^-	3197.7	5^-	$E2$	2345.2	5.3		
		3708.4	5^-	$E2$	1834.6	5.0		
		3919.9	6^-	$M1$	1623.1	5.1	6.1	1.8
		3961.1	5^-	$E2$	1581.9	2.1		
		4037.6	7^-	$M1$	1505.4	7.6	10.8	1.8
		4206.3	6^-	$M1$	1336.7	17.0	18.3	2.0
		4383.3	6^-	$M1$	1159.7	41.6	42.7	3.4
		4480.8	6^-	$M1$	1062.2	2.9	6.9	1.0
		5085.5	7^-	$M1$	457.5	10.9	12.3	1.4
$T_{1/2}=0.26E-13s$								
5695.0	7^-	3919.9	6^-	$M1$	1775.1	89.0	100.0	
		4037.6	7^-	$M1$	1657.4	3.8		
		4206.3	6^-	$M1$	1488.6	1.1		
		4383.3	6^-	$M1$	1311.7	1.3		
		5085.5	7^-	$M1$	609.5	1.5		
$T_{1/2}=0.15E-13s$								
4867.8	7^+	4423.5	6^+	$M1$	444.3	31.3	29.5	5.9
		4423.5	6^+	$E2$	444.3	1.1		
		4610.9	8^+	$M1$	256.9	67.7	30.8	4.6

TABLE II. (*Continued*).

Init.		Final		Λ	E_γ	b_{th}	b_{exp}	Err.
$T_{1/2}=0.12E-10s$								
5195.4	7^+	4423.5	6^+	$M1$	771.8	76.2	76.3	10.7
		4423.5	6^+	$E2$	771.8	7.2		
		4610.9	8^+	$M1$	584.4	0.1	0.0	0.0
		4860.9	8^+	$M1$	334.4	3.1	2.0	0.7
		4867.8	7^+	$M1$	327.6	13.0	14.3	1.7
$T_{1/2}=0.69E-12s$								
610.9	8^+	4423.5	6^+	$E2$	187.4	100.0		
$T_{1/2}=0.33E-05s$								
4860.9	8^+	4610.9	8^+	$M1$	250.0	99.9	74.0	7.7
$T_{1/2}=0.28E-11s$								
5093.2	8^+	4610.9	8^+	$M1$	482.3	82.7	93.5	8.3
		4860.9	8^+	$M1$	232.3	17.2	6.5	2.4
$T_{1/2}=0.17E-12s$								
5339.6	8^+	4610.9	8^+	$M1$	728.6	62.6	52.9	5.9
		4860.9	8^+	$M1$	478.6	33.1	33.6	4.2
		5093.2	8^+	$M1$	246.4	3.9		
$T_{1/2}=0.11E-12s$								
5826.2	8^+	4610.9	8^+	$M1$	1215.3	74.7	100.0	
		4860.9	8^+	$M1$	965.3	7.8		
		4867.8	7^+	$M1$	958.4	4.4		
		5093.2	8^+	$M1$	733.0	10.3		
		5339.6	8^+	$M1$	486.6	1.8		
$T_{1/2}=0.17E-13s$								
5010.7	9^+	4610.9	8^+	$M1$	399.7	80.6	96.4	6.7
		4610.9	8^+	$E2$	399.7	5.2		
		4860.9	8^+	$M1$	149.7	6.6		
		4895.4	10^+	$M1$	115.3	7.4	3.6	1.0
$T_{1/2}=0.15E-09s$								
5162.2	9^+	4610.9	8^+	$M1$	551.3	39.7	54.0	4.3
		4610.9	8^+	$E2$	551.3	3.1		
		4860.9	8^+	$M1$	301.3	10.4	11.8	1.8
		4895.4	10^+	$M1$	266.8	5.5	9.0	1.6
		5010.7	9^+	$M1$	151.6	40.6	25.1	2.6
$T_{1/2}=0.32E-11s$								
895.4	10^+	4610.9	8^+	$E2$	284.5	99.9	83.8	7.4
		4860.9	8^+	$E2$	34.5	0.1	0.0	0.0
$T_{1/2}=0.14E-05s$								
5069.5	10^+	4895.4	10^+	$M1$	174.1	100.0	100.0	0.0
$T_{1/2}=0.12E-11s$								
5536.7	10^+	4895.4	10^+	$M1$	641.3	79.1	81.2	9.1
		5069.5	10^+	$M1$	467.2	20.5	18.8	4.8
$T_{1/2}=0.51E-13s$								
5928.3	10^+	4895.4	10^+	$M1$	1032.9	60.0	64.8	8.2
		5069.5	10^+	$M1$	858.8	38.3	35.2	12.6
		5536.7	10^+	$M1$	391.6	1.1		
$T_{1/2}=0.16E-13s$								
5235.6	11^+	4895.4	10^+	$M1$	340.2	91.3	100.0	0.0
		4895.4	10^+	$E2$	340.2	5.9		
		5069.5	10^+	$M1$	166.0	2.7		
$T_{1/2}=0.93E-10s$								
5749.0	11^+	4895.4	10^+	$M1$	853.6	21.1	22.0	10.0
		5069.5	10^+	$M1$	679.5	74.0	78.0	10.0
		5069.5	10^+	$E2$	679.5	2.2		
		5235.6	11^+	$M1$	513.4	1.4		
$T_{1/2}=0.37E-11s$								
6100.9	12^+	5235.6	11^+	$M1$	865.4	74.0	80.0	5.0
		5235.6	11^+	$E2$	865.4	1.2		
		5749.0	11^+	$M1$	351.9	23.3	20.0	5.0
$T_{1/2}=0.44E-11s$								

TABLE III. Transition amplitudes for the decay $6_1^- \rightarrow 5_1^-$. The columns labelled $M1$ and $E2$ give the transition matrix elements for the configurations of column 1. The corresponding transition amplitudes (labelled Amplitude) include the amplitudes of the configurations in the two states.

Transition	$M1$ (nm)	Amplitude (nm)	$E2$ (e fm^2)	Amplitude (e fm^2)
$(\nu g_{9/2} f_{5/2}^{-1};\ 6^-) \rightarrow (\nu g_{9/2} f_{5/2}^{-1};\ 5^-)$	1.84	−0.28	44.6	−6.7
$(\nu g_{9/2} f_{5/2}^{-1};\ 6^-) \rightarrow (\nu g_{9/2} p_{1/2}^{-1};\ 5^-)$	0.	0	−25.7	24.5
$(\nu g_{9/2} p_{3/2}^{-1};\ 6^-) \rightarrow (\nu g_{9/2} p_{1/2}^{-1};\ 5^-)$	−2.31	0.07	−14.9	0.4

branch from 4_3^- to 5_1^- would not be reproduced. In this way, the wave functions of the 6^- and 4^- states are indirectly connected. This shows the interdependence of nearly all amplitudes of all states.

Finally little is known about the $\nu 1i_{11/2} 2f_{5/2}^{-1}$ component, except that the absence of a transition from 6_5^- limits its amplitude squared to about 0.1. In general this configuration is only poorly determined, because it is not connected to any other configuration by a strong transition element.

The two main components of the second and third 6^- states $\nu 1i_{11/2} 3p_{1/2}^{-1}$ and $\pi 1h_{9/2} 2d_{3/2}^{-1}$ are determined by the spectroscopic factors. This agrees also fully with the decays from 7_3^- and 7_4^-; these levels have as main components $\nu i1_{11/2} 3p_{3/2}^{-1}$ and $\pi 1h_{9/2} 2d_{5/2}^{-1}$. The holes are the spin-orbit partners of the holes in the 6^- states and consequently the $M1$ matrix elements are strong and govern these decays. Again the $\nu 2g_{9/2} 2f_{5/2}^{-1}$ and $\nu 2g_{9/2} 3p_{3/2}^{-1}$ components of the 6^- states influence the branching to the lower states strongly.

The main component of the fourth 6^- level is $\nu 2g_{9/2} 3p_{3/2}^{-1}$ leading to a dominant decay to 5_1^-. But all ten transition matrix elements, except one, interfere constructively to give a measurable branch to 5_2^-. This makes the smaller components of the wave function believable. The transfer of an $1i_{11/2}$ neutron is weak in (d,p) and cannot be detected for the deduced spectroscopic factor $S=0.01$. The wave function of the fifth 6^- level should not be taken too seriously.

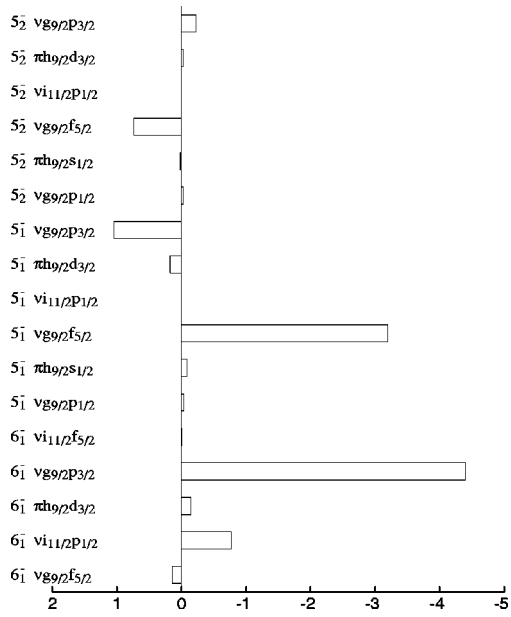

FIG. 2. Partial derivative of the relative strength of the transition from the first 6^--level to the first 5^--level with respect to the amplitudes of the indicated wave functions.

The spectroscopic factors and γ branching ratios are well reproduced for the 5 lowest 7^- states. The only shortcoming are the predicted $E2$ branches from 7_4^- to the two lowest 5-levels. The 7^- and 6^- states are very little mixed and consequently perturbation theory should be adequate. It predicts $a_{i,k} = -a_{k,i}$ for the nondiagonal amplitudes of the wave functions. This is well satisfied in both cases (Table I).

F. The positive parity states with odd spin

The ^{209}Bi$(t,\alpha\gamma)^{208}$Pb reaction populates only one state each with $I^\pi = 3^+, 5^+, 7^+$; a second 9^+ level is populated with 3% of the main proton state. Therefore these unnatural parity states are practically pure $\pi 1h_{9/2} 1h_{11/2}^{-1}$. The tentative spin assignment for the 3^+ level is based on its strength in proton pick up and the γ decay to 4^+ and 3^-. The γ branching from the 5^+ level to the lowest 4^+ and 6^+ states is very well reproduced. It depends only on the amplitudes of the $\pi 1h_{9/2} 1h_{11/2}^{-1}$ configuration in these states. These are also independently measured by the spectroscopic factors. Therefore this is a direct proof for the consistency of the information from the reaction cross sections and the γ decay.

Two 7^+ levels have been identified. There is no evidence for the third state of mainly the configuration $\nu 2g_{9/2} 1i_{13/2}^{-1}$, which is expected between the two others. As this prevents the orthonormalization of the wave functions the interpretation of the data is less strict. The γ branching of the lower 7^+ level is reasonably reproduced, considering that all transitions are weak. The very good agreement for the higher 7^+ level requires a subtle interference from the three configurations. With just one free parameter the spectroscopic factors and the γ decay of the two 9^+ states are well reproduced.

There is no experimental evidence yet for the lowest 3^+ and 5^+ and the second 7^+ state, that belong mainly to the configuration $\nu 2g_{9/2} 1i_{13/2}^{-1}$. Evidently they mix so little with the proton configuration, that they are not excited.

G. The positive parity states with even spin

The 0^+ and 2^+ states are not considered here. The 4^+ levels decay primarily by $E1$ transitions. Therefore the only information on their structure is the $\pi 1h_{9/2} 1h_{11/2}^{-1}$ strength from the spectroscopic factors, and wave functions cannot be derived. The spin of the 5239.4 keV level is not determined, but, of the few expected and not yet assigned levels around this energy, the 4^+ member of the double octupole phonon excitation could explain the measured data. It would be

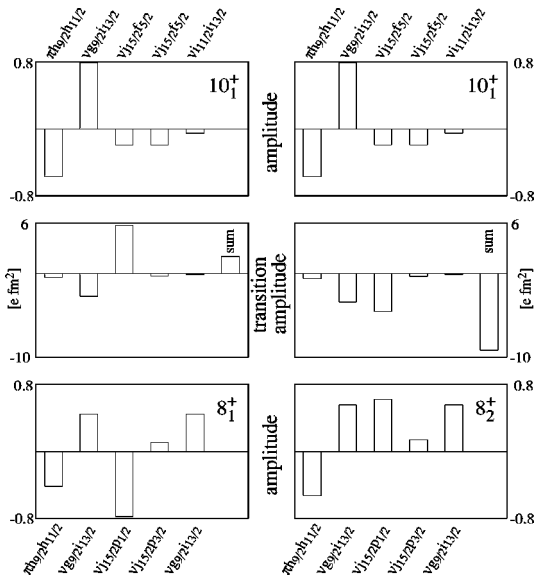

FIG. 3. The figure shows the amplitudes of the configurations of the 10_1^+ state on top and those of the two 8^+ states on the bottom. In the middle the corresponding $E2$-transition elements are shown. The different signs of the $\nu j_{15/2}p_{1/2}^{-1}$ configuration in the 8^+ states lead to destructive or constructive interference.

strongly mixed with the nearly degenerate $\pi 1h_{9/2}1h_{11/2}^{-1}$ 4^+ level at 5216.5 keV. Yeh *et al.* [12] favor the 5216.5 keV state as double octupole. The next possible particle-hole configuration for a 4^+ state $\nu 1i_{11/2}1i_{13/2}^{-1}$ lies about 600 keV higher.

Again just one mixing parameter for the two 6^+ levels describes the strength of the $1h_{11/2}$ proton pick up and the γ branching into them from the 5^+ and 7^+ levels well.

Five 8^+ and four 10^+ levels have been identified. A sixth 8^+ level is expected close by; but the four 10^+ levels are well separated from the next higher state. In both cases the $\pi 1h_{9/2}1h_{11/2}^{-1}$ strength is distributed fairly uniformly. The lowest 8^+ state shows a half-life of $T_{1/2}=3.2(5)$ ns. This is exactly reproduced for the decay from its $\nu 1j_{15/2}3p_{1/2}^{-1}$ component ($a=-0.78$) to the pure $\nu 2g_{9/2}3p_{1/2}^{-1}$ 5_1^- state with the known $B(E3,\nu 1j_{15/2}\rightarrow 2g_{9/2})=22$W.u. The γ decay agrees therefore with the spectroscopic factor of the neutron transfer reaction. An analogous $E3$ transition proceeds also from the weak ($a=-0.19$) $\nu 1j_{15/2}2f_{5/2}^{-1}$ component of the lowest 10^+ level to the practically pure $\nu 2g_{9/2}2f_{5/2}^{-1}$ 7_1^- level. Figure 3 shows the wave functions of the 10_1^+ and $8_{1,2}^+$ levels and the transition-matrix elements of the connecting $E2$ transitions. The destructive interference of the $\nu 2g_{9/2}1i_{13/2}^{-1}$ to $\nu 2g_{9/2}1i_{13/2}^{-1}$ and $\nu 1j_{15/2}2f_{5/2}^{-1}$ to $\nu 1j_{15/2}3p_{1/2}^{-1}$ contributions for the 8_1^+ state give rise to the long half-life ($T_{1/2}=500$ ns) of the 10^+ state [18]. The $E2$ transitions from the 10^+ level determine the amplitudes of the $\nu 2g_{9/2}1i_{13/2}^{-1}$ configuration in the two lowest 8^+ levels, and together with the two measured spectroscopic factors the three important components are fixed.

For the 10^+ states the $\pi 1h_{9/2}1h_{11/2}^{-1}$ configuration is known from the proton pick up. The $\nu 2g_{9/2}1i_{13/2}^{-1}$ and $\nu 1j_{15/2}2f_{5/2}^{-1}$ configurations for 10_1^+ have already been discussed in connection with the decay to the 8^+ states. $\nu 2g_{9/2}1i_{13/2}^{-1}$ is in addition sensitive to the $M1$ branchings from the higher lying 10^+ levels. Finally the amplitude of the $\nu 1i_{11/2}1i_{13/2}^{-1}$ configuration is very sensitive to the decay from 11_2^+, as its wave function is pure $\nu 1i_{11/2}1i_{13/2}^{-1}$. All 4 possible configurations are therefore well measured for the first 10^+ state. There is however no direct evidence on the amplitudes of the $\nu 1j_{15/2}2f_{5/2}^{-1}$ and $\nu 1i_{11/2}1i_{13/2}^{-1}$ configurations in the two highest 10^+ levels. They are only determined from the orthonormality requirement.

H. States with spin 11 to 14

The highest spin that can be formed by one particle one hole configurations is 14^-. The wave function of the 14^- level is pure $\nu 1j_{15/2}1i_{13/2}^{-1}$, because no other configuration is possible. This holds also for the 13^- state. The 12^+ level can likewise only be $\nu 1i_{11/2}1i_{13/2}^{-1}$. Two 11^+ levels have been found [19] with the pure configurations $\nu 2g_{9/2}1i_{13/2}^{-1}$ and $\nu 1i_{11/2}1i_{13/2}^{-1}$ [19]. Primarily the absence of a γ branch from 11_2^+ to 11_1^+ excludes appreciable configuration mixing. Therefore all the known states with spin above 10 have pure configurations.

I. General remarks on the wave functions

It has been possible to describe many levels of ^{208}Pb with one particle–one hole wave functions. In particular the amplitudes as measured by transfer reactions agree well with those determined from the γ transitions. The measured spectroscopic factors have been normalized such, that sum $(S_i)=1$ for a given transferred j and I^π of final states. The wave functions are orthonormal, as they should be for an adequate model. Much qualitative information on the neutron particle-hole structure of many states has also been gained from inelastic proton scattering through analog states [20]. The deduced wave functions agree with this.

No need arose to include any two particle two hole configurations or ''collective'' contributions for the considered states. On the other hand excited 0^+ states can only be formed by two particle two hole excitations, and these excitations contribute significantly to the 2^+ and also 4^+, 6^+ levels.

The use of effective $M1$ and $E2$ matrix elements means however that special more complicated admixtures are present. It is well known, for example, that the differences between the Schmidt values and the measured magnetic moments of the single particle orbitals are in part caused by magnetic core polarization. These are admixed 1^+ excitations of the ^{208}Pb core, that are too weak to noticeably influence any other properties but $M1$. It might well be, that the Y_5 collectivity of the lowest 5^- level, that is evident in inelastic proton scattering [21], is caused by other small admixtures, which do not influence the properties considered in our analysis.

The γ-transition rates result from the coherent superposition of the transition amplitudes and determine therefore the signs of the amplitudes. But of course a simultaneous change of corresponding signs in the initial and final state gives the same transition strength. Because the signs are however mostly also fixed by some other γ transition and by the orthonormality requirement, it is unlikely that individual signs are wrong. But the signs of whole groups of amplitudes

TABLE IV. Matrix elements of the residual interaction, as calculated from level energies and wave functions. The diagonal proton elements are corrected for Coulomb pairing by +300 keV. In addition to the table there are the following diagonal elements: $\langle \nu 1i_{11/2}1i_{13/2}^{-1};12^+|H|\nu 1i_{11/2}1i_{13/2}^{-1};12^+\rangle = 258$ keV; $\langle \nu 1j_{15/2}1i_{13/2}^{-1};13^-|H|\nu 1j_{15/2}1i_{13/2}^{-1};13^-\rangle = -38$ keV; $\langle \nu 1j_{15/2}1i_{13/2}^{-1};14^-|H|\nu 1j_{15/2}1i_{13/2}^{-1};14^-\rangle = 257$ keV.

			0^- states			
Configuration	$\nu 4s_{1/2}3p_{1/2}^{-1}$	$\nu 3d_{5/2}2f_{5/2}^{-1}$				
$\nu 4s_{1/2}3p_{1/2}^{-1}$	−139	110				
$\nu 3d_{5/2}2f_{5/2}^{-1}$	110	−12				
			1^- states			
Configuration	$\nu 4s_{1/2}3p_{1/2}^{-1}$	$\nu 3d_{5/2}2f_{5/2}^{-1}$	$\nu 2g_{9/2}2f_{7/2}^{-1}$			
$\nu 4s_{1/2}3p_{1/2}^{-1}$	−136	-82	5			
$\nu 3d_{5/2}2f_{5/2}^{-1}$	−83	−127	−147			
$\nu 2g_{9/2}2f_{7/2}^{-1}$	0	−143	−894			
			2^- states			
Configuration	$\nu 2g_{9/2}2f_{5/2}^{-1}$	$\nu 3d_{5/2}3p_{1/2}^{-1}$	$\pi 2f_{7/2}2d_{3/2}^{-1}$			
$\nu 2g_{9/2}2f_{5/2}^{-1}$	317	−218	133			
$\nu 3d_{5/2}3p_{1/2}^{-1}$	−215	5	82			
$\pi 2f_{7/2}2d_{3/2}^{-1}$	128	81	−88			
			4^- states			
Configuration	$\nu 2g_{9/2}3p_{1/2}^{-1}$	$\pi 1h_{9/2}3s_{1/2}^{-1}$	$\nu 2g_{9/2}2f_{5/2}^{-1}$	$\pi 1h_{9/2}2d_{3/2}^{-1}$	$\nu 2g_{9/2}3p_{3/2}^{-1}$	
$\nu 2g_{9/2}3p_{1/2}^{-1}$	99	−46	75	−41	−171	
$\pi 1h_{9/2}3s_{1/2}^{-1}$	−38	68	3	−109	−11	
$\nu 2g_{9/2}2f_{5/2}^{-1}$	86	8	−4	−26	−42	
$\pi 1h_{9/2}2d_{3/2}^{-1}$	−76	−114	−22	−19	25	
$\nu 2g_{9/2}3p_{3/2}^{-1}$	−174	−20	−47	30	−46	
			5^- states			
Configuration	$\nu 2g_{9/2}3p_{1/2}^{-1}$	$\pi 1h_{9/2}3s_{1/2}^{-1}$	$\nu 2g_{9/2}2f_{5/2}^{-1}$	$\nu 1i_{11/2}3p_{1/2}^{-1}$	$\pi 1h_{9/2}2d_{3/2}^{-1}$	$\nu 2g_{9/2}3p_{3/2}^{-1}$
$\nu 2g_{9/2}3p_{1/2}^{-1}$	−182	148	−76	33	−38	−3
$\pi 1h_{9/2}3s_{1/2}^{-1}$	154	−59	121	88	−113	−21
$\nu 2g_{9/2}2f_{5/2}^{-1}$	−72	118	−151	−87	48	5
$\nu 1i_{11/2}3p_{1/2}^{-1}$	38	92	−89	−44	−25	45
$\pi 1h_{9/2}2d_{3/2}^{-1}$	−38	−116	49	−27	−135	−60
$\nu 2g_{9/2}3p_{3/2}^{-1}$	−5	−17	5	43	−58	−109
			6^- states			
Configuration	$\nu 2g_{9/2}2f_{5/2}^{-1}$	$\nu 1i_{11/2}3p_{1/2}^{-1}$	$\pi 1h_{9/2}2d_{3/2}^{-1}$	$\nu 2g_{9/2}3p_{3/2}^{-1}$	$\nu 1i_{11/2}2f_{5/2}^{-1}$	
$\nu 2g_{9/2}2f_{5/2}^{-1}$	−77	3	−43	−1	−2	
$\nu 1i_{11/2}3p_{1/2}^{-1}$	3	6	−43	−1	−2	
$\pi 1h_{9/2}2d_{3/2}^{-1}$	−45	−40	132	−26	−14	
$\nu 2g_{9/2}3p_{3/2}^{-1}$	−14	25	−27	153	53	
$\nu 1i_{11/2}2f_{5/2}^{-1}$	0	7	−15	53	−29	
			6^+ states			
Configuration	$\nu 2g_{9/2}1i_{13/2}^{-1}$	$\pi 1h_{9/2}1h_{11/2}^{-1}$				
$\nu 2g_{9/2}1i_{13/2}^{-1}$	−502	−300				
$\pi 1h_{9/2}1h_{11/2}^{-1}$	−300	−188				
			7^- states			
Configuration	$\nu 2g_{9/2}2f_{5/2}^{-1}$	$\nu 1i_{11/2}2f_{5/2}^{-1}$	$\nu 1i_{11/2}3p_{3/2}^{-1}$	$\pi 1h_{9/2}2d_{5/2}^{-1}$	$\nu 2g_{9/2}2f_{7/2}^{-1}$	
$\nu 2g_{9/2}2f_{5/2}^{-1}$	52	0	−1	2	−156	
$\nu 1i_{11/2}2f_{5/2}^{-1}$	0	−100	0	0	0	
$\nu 1i_{11/2}3p_{3/2}^{-1}$	3	0	22	−137	13	
$\pi 1h_{9/2}2d_{5/2}^{-1}$	−40	0	−139	−85	−45	
$\nu 2g_{9/2}2f_{7/2}^{-1}$	−163	0	14	−42	−105	
			8^+ states			
Configuration	$\nu 1j_{15/2}3p_{1/2}^{-1}$	$\nu 2g_{9/2}1i_{13/2}^{-1}$	$\pi 1h_{9/2}1h_{11/2}^{-1}$	$\nu 1j_{15/2}2f_{5/2}^{-1}$	$\nu 1j_{15/2}3p_{3/2}^{-1}$	
$\nu 1j_{15/2}3p_{1/2}^{-1}$	−146	87	−83	0	22	
$\nu 2g_{9/2}1i_{13/2}^{-1}$	87	−106	189	75	−49	
$\pi 1h_{9/2}1h_{11/2}^{-1}$	−82	189	−280	73	78	
$\nu 1j_{15/2}2f_{5/2}^{-1}$	0	76	74	−146	−19	
$\nu 1j_{15/2}3p_{3/2}^{-1}$	21	−50	78	−19	−490	

TABLE IV. (*Continued*).

		9^+ states		
Configuration	$\nu 2g_{9/2}1i_{13/2}^{-1}$	$\pi 1h_{9/2}1h_{11/2}^{-1}$		
$\nu 2g_{9/2}1i_{13/2}^{-1}$	−47	−30		
$\pi 1h_{9/2}1h_{11/2}^{-1}$	−30	−106		
		10^+ states		
Configuration	$\nu 2g_{9/2}1i_{13/2}^{-1}$	$\pi 1h_{9/2}1h_{11/2}^{-1}$	$\nu 1j_{15/2}2f_{5/2}^{-1}$	$\nu 1i_{11/2}1i_{13/2}^{-1}$
$\nu 2g_{9/2}1i_{13/2}^{-1}$	8	194	179	−93
$\pi 1h_{9/2}1h_{11/2}^{-1}$	193	−96	58	−262
$\nu 1j_{15/2}2f_{5/2}^{-1}$	176	58	−15	166
$\nu 1i_{11/2}1i_{13/2}^{-1}$	−93	−261	166	−61
		11^+ states		
Configuration	$\nu 2g_{9/2}1i_{13/2}^{-1}$	$\nu 1i_{11/2}1i_{13/2}^{-1}$		
$\nu 2g_{9/2}1i_{13/2}^{-1}$	171	0		
$\nu 1i_{11/2}1i_{13/2}^{-1}$	0	−93		

could perhaps be changed. There is for instance no γ transition between a neutron and a proton configuration, and therefore the sign of all proton amplitudes in all states might be changed simultaneously. The γ transitions do not determine the sign for the $\pi 1h_{9/2}1h_{11/2}^{-1}$ configuration in the 10^+ levels either. It is taken from inelastic electron scattering [22]. There might be other not quite so evident cases, that have to be checked if a serious doubt results from other data.

The agreement between our empirical wave functions and those calculated by True *et al.* [2] for negative parity states with a phenomenological interaction is remarkably good for the lower states. There are however also significant differences, that might perhaps be used to improve their force. Our empirical wave functions are limited to the lowest configurations. The calculated [2] wave functions include also higher configurations. That these are really present, although small, is proven by the measurement of $^{207}\mathrm{Pb}(d,p)^{208}\mathrm{Pb}$ with polarized deuterons [13]. It shows mixing between $3d_{3/2}$ and $3d_{5/2}$ orbitals.

III. THE RESIDUAL INTERACTION

A. Derivation of the residual interaction

The Schrödinger equation $H\psi = E\psi$ is usually interpreted as an eigenvalue equation; the Hamiltonian matrix H is known and the energies E and wave functions ψ are to be calculated. Here we regard it as a system of linear equations to calculate the elements of the Hamiltonian from the measured level energies and the wave functions. The results are presented in Table IV. The diagonal matrix elements include the residual interaction only, the single particle energies as given in Fig. 1 have been subtracted. Also the presented diagonal elements for all proton configurations show the directly calculated values plus 300 keV. This compensates that the energies of the proton particle-hole configurations are lowered by a roughly constant amount of 300 keV due to the Coulomb pairing interaction. As presented, the residual interaction for protons and neutrons is comparable.

B. Discussion of the residual interaction

1. Nondiagonal elements

The main discussion below is restricted to the diagonal matrix elements, as they can be presented in a perceptual way. For the nondiagonal elements no meaningful representation as a function of few parameters is known as they depend on 4 orbitals and the spin of the state. There are no calculated and published nondiagonal matrix elements available either for a direct comparison. This is unfortunate as the nondiagonal elements are essentially new information; diagonal elements have been deduced and interpreted for neighboring nuclei before, disregarding configuration mixing, see, e.g., Ref. [23]. A difficulty in the interpretation of all matrix elements is, that the particle-particle formalism is normally used in theory, while our analysis uses the particle-hole formalism, as dictated from the nature of the data. The Pandya transformation converts from on to the other scheme, but requires a complete set of matrix elements for all spins to which the participating orbitals can couple. Therefore the transformation is often not possible. As mentioned above there is some uncertainty of the signs in the wave functions, that gives an uncertainty of the sign of the corresponding nondiagonal matrix elements. In a comprehensive treatment these limited uncertainties can be resolved, and as soon as a consistent and complete set of theoretical interactions becomes available, a comparison should be made. The offdiagonal elements are usually small ($\sim$100 keV) and markedly smaller for unnatural than for natural parity states.

2. Diagonal elements

The diagonal matrix elements can be graphically presented in a meaningful way as in Figs. 4(a)–4(c). These figures show also approximate errors of the interaction energies, as derived from the errors of the amplitudes of the wave functions [9]. A classical angle Θ between the spins of the interacting particle j_p and hole j_h in a state I^π is defined as

$$\Theta = \arccos\left[\frac{I(I+1)-j_p(j_p+1)-j_h(j_h+1)}{2\sqrt{j_p(j_p+1)j_h(j_h+1)}}\right].$$

For approximately parallel (maximal I) or antiparallel (minimal I) spins the planes, in which the particle and hole move, overlap well, and a large interaction energy is expected for an interaction of short range. At intermediate spins the overlap is small. Therefore the matrix elements should roughly lie on a parabola, if plotted against Θ. The

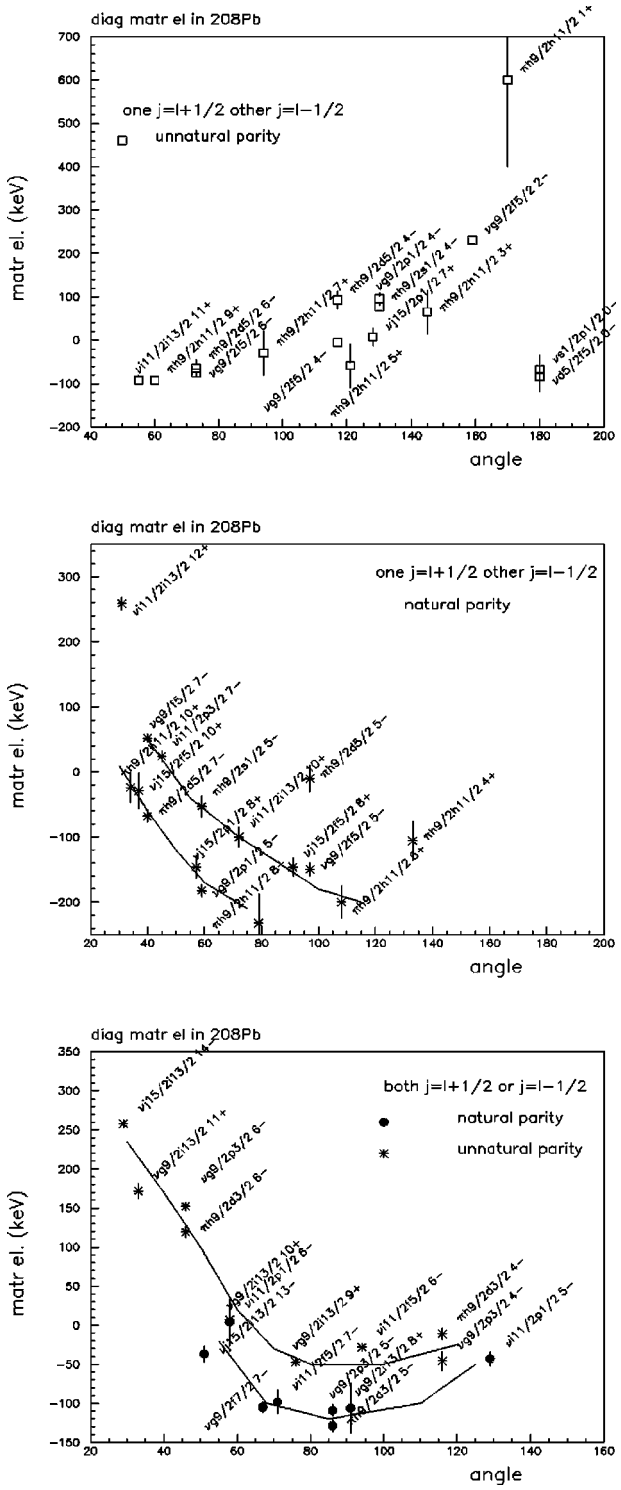

FIG. 4. Diagonal matrix elements of the residual shell model interaction between particles and holes in ^{208}Pb as functions of the classical angle between the angular momenta. The lines are to guide the eye only. (a) Levels of unnatural parity, if $j=l+1/2$ for the particle then $j=l-1/2$ for the hole or vice versa. (b) Levels of natural parity, if $j=l+1/2$ for the particle then $j=l-1/2$ for the hole or vice versa. (c) $j=l+1/2$ or $j=l-1/2$ for both particle and hole.

advantage of this representation is that all matrix elements can be shown together irrespective of the detailed quantum numbers of the orbits. As Figs. 4(a)–4(c) show, the matrix elements follow indeed the expected trend versus the angle Θ. Two further distinctions are important. The empirical matrix elements show a marked difference depending if the Nordheim number $j_p+j_h+l_p+l_h$ is even or odd; in other words there is a distinction between the two cases: (i) spin and orbital angular momentum are either parallel or antiparallel for both particle and hole or (ii) they are parallel for one and antiparallel for the other. Also the classification between natural $\pi=(-1)^I$ and unnatural $\pi=-(-1)^I$ parity of the state is important; the diagonal matrix elements are larger for natural parity states. This accords with the clearly larger nondiagonal elements for natural parity.

The interaction in the unnatural parity states of odd Nordheim number [Fig. 4(a)] is weak, between +100 and −100 keV and shows no dependence on angle over the range from 50 to 180°. An exception is the 1^+ state. States of similar nature have mostly the same interaction energy; examples are $(\nu 1i_{11/2}1i_{13/2}^{-1};11^+)$ and $(\pi 1h_{9/2}1h_{11/2}^{-1};9^+)$ or $(\nu g2_{9/2}2f_{5/2}^{-1};6^-)$ and $(\pi 1h_{9/2}2d_{5/2}^{-1};6^-)$ or $(\nu 2g_{9/2}3p_{1/2}^{-1};4^-)$ and $(\pi 1h_{9/2}3s_{1/2}^{-1};4^-)$.

For odd Nordheim number and natural parity [Fig. 4(b)] only angles from 30 to 110° are covered. The interaction energy drops from about 0 keV at small angles to −200 keV around 90°. This is the expected general dependence on angle. It is tempting to group the data into two groups as indicated by the lines in the figure. But we could not recognize any distinction between the structure of the states in these two groups. Three matrix elements are rather different from all others.

The matrix elements for even Nordheim number [Fig. 4(c)] exhibit rather clearly a parabolic dependence on angle, and there is a marked difference between natural and unnatural parity. Again the interaction energies for the similar configurations $\nu 2g_{9/2}3p_{3/2}^{-1}$ and $\pi 1h_{9/2}2d_{3/2}^{-1}$ are nearly equal for spin 4, 5, and 6.

All matrix elements of the residual interaction are rather small, only few exceed 200 keV. The fact, that reasonable trends can be seen at all, supports the validity of the presented analysis. The dependence on the classical angle, means that the interaction is of short range. The radial wave functions are of little influence, although orbitals with between 0 and 3 radial nodes are present; this indicates that the interaction is concentrated in the surface, as the amplitudes of the wave functions at the surface of the nucleus change only little with radial quantum number.

Moinester, Schiffer, and Alford [23] analyzed the diagonal matrix elements of the interaction between protons and neutrons in ^{210}Bi and protons and neutron holes in ^{208}Bi from measured energies and assuming pure configurations. They used a multipole expansion of the interaction energies. The energy of a state is given as

$$E_I(j_1j_2)=\sum_k \alpha^k_{j_1j_2}E^k_I(j_1j_2).$$

The quantities $E^k_I(j_1j_2)$ depend only on angular momenta, while the expansion coefficients $\alpha^k_{j_1j_2}$ really determine the interaction. They showed, that the $\alpha^k_{j_1j_2}/\alpha^0_{j_1j_2}$ are approximately independent of the individual orbitals. This means that the interaction is primarily determined by the angular momenta. The same conclusion has been reached above by

TABLE V. Reduced $M1$ and $E2$ matrix elements in nm and e fm^2, as used in the present analysis. This is an updated version of the table by Donahue *et al.* [31]; some signs have been corrected. The references for more recent values are indicated. See also the text.

from	to	$M1$	Ref.	$E2$	Ref.	from	to	$M1$	Ref.	$E2$	Ref.
		Proton particles						Proton holes			
$1h_{9/2}$	$1h_{9/2}$	6.97(15)		−55.9(5)	[32]	$3s^{-1}_{1/2}$	$3s^{-1}_{1/2}$	2.25(1)	[33]	0.00	
$1h_{9/2}$	$2f_{7/2}$	0.18		-15.50		$2d^{-1}_{3/2}$	$3s^{-1}_{1/2}$	0.30	[34]	33.50	
$2f_{7/2}$	$2f_{7/2}$	8.08	[35]	−53.50	[36]	$2d^{-1}_{5/2}$	$3s^{-1}_{1/2}$	0.00		37.10	[36]
$1i_{13/2}$	$1i_{13/2}$	15.71(30)		−66(16)	[32]	$2d^{-1}_{3/2}$	$2d^{-1}_{3/2}$	0.96	[34]	29.60	[36]
						$2d^{-1}_{5/2}$	$2d^{-1}_{3/2}$	1.90	[34]	−20.50	[36]
						$1h^{-1}_{11/2}$	$1h^{-1}_{11/2}$	12.78(27)	[37]	75(11)	[38]
						$2d^{-1}_{5/2}$	$2d^{-1}_{5/2}$	5.93	[34]	40.10	[36]
		Neutron particles						Neutron holes			
$2g_{9/2}$	$2g_{9/2}$	−2.42(12)	[39]	−39(2)	[39]	$3p^{-1}_{1/2}$	$3p^{-1}_{1/2}$	0.71		0.00	
$2g_{9/2}$	$1i_{11/2}$	0.35		6.90		$2f^{-1}_{5/2}$	$3p^{-1}_{1/2}$	0.00		20.60	
$1i_{11/2}$	$1i_{11/2}$	1.07	[34]	−39.30	[36]	$3p^{-1}_{3/2}$	$3p^{-1}_{1/2}$	−1.28		−15.60	
$1j_{15/2}$	$1j_{15/2}$	−2.68(20)	[34]	−64.00	[36]	$2f^{-1}_{5/2}$	$2f^{-1}_{5/2}$	1.08(3)		25.90	[36]
$2g_{9/2}$	$3d_{5/2}$	0.00		−32.90		$3p^{-1}_{3/2}$	$2f^{-1}_{5/2}$	0.44		−11.20	
$3d_{5/2}$	$3d_{5/2}$	−1.90		−18.10	[36]	$2f^{-1}_{7/2}$	$2f^{-1}_{5/2}$	−1.98		−11.70	
$3d_{5/2}$	$4s_{1/2}$	0.00		−17.70		$3p^{-1}_{3/2}$	$3p^{-1}_{3/2}$	−1.60		16.90	[36]
$4s_{1/2}$	$4s_{1/2}$	−1.47	[34]	0.00		$2f^{-1}_{7/2}$	$3p^{-1}_{3/2}$	0.00		27.70	
$3d_{5/2}$	$3d_{3/2}$	−1.63		9.40		$1i^{-1}_{13/2}$	$1i^{-1}_{13/2}$	−1.96(5)	[40]	48.6	[41]
$4s_{1/2}$	$3d_{3/2}$	0.00	[42]	14.10		$2f^{-1}_{7/2}$	$2f^{-1}_{7/2}$	−2.01		48.50	
$3d_{3/2}$	$3d_{3/2}$	1.12	[34]	−14.10	[36]						
$2g_{9/2}$	$2g_{7/2}$	−1.96	[34]	11.70							
$1i_{11/2}$	$2g_{7/2}$	0.00		−40.00							
$3d_{5/2}$	$2g_{7/2}$	0.00	[42]	6.90							
$3d_{3/2}$	$2g_{7/2}$	0.00		−23.20							
$2g_{7/2}$	$2g_{7/2}$	1.49	[34]	−31.30	[36]						

the observation, that the matrix elements exhibit clear trends as a function of the classical angle and roughly independent of the radial quantum numbers. Moinester *et al.* [23] also found a marked influence of the Nordheim number, namely that the α_k with odd k change sign according to the Nordheim number. This multipole expansion connects also the particle-hole interaction with the particle-particle (or hole-hole) interaction simply by a change of sign for the α_k with even k. A short trial, to see if also our ^{208}Pb data agree with the general interaction of Ref. [23], was inconclusive.

IV. CONCLUSIONS

Shell-model wave functions of many states in ^{208}Pb have been derived from measured data empirically. This became possible by a reliable and sufficiently complete set of data [10]. It would be very interesting to check if these wave functions also reproduce other measured data, like inelastic electron scattering [24], that is sensitive to other aspects of the structure. Knowledge of the structure of the states of ^{208}Pb is also necessary to understand neighboring nuclei, in which few particles couple to the levels of ^{208}Pb.

The region around ^{208}Pb is so attractive, as it is beyond ^{48}Ca the only stable doubly magic nucleus. As also the neighbors ^{207}Pb and ^{209}Bi are stable a large variety of reactions can be studied and a rather complete picture of the structure formed. Excellent experiments with radioactive beams and targets, like $^{210m}\mathrm{Bi}(t,\alpha)^{209}$Pb, that are impossible now, have been performed long ago [25]. Until recently information on γ decays had been scarce due to a lack of suitable reactions. But better detectors have overcome these problems. Coincidences between charged particles and γ rays have been measured [10], very good γ spectra obtained with (n,n') [11], the (d,p) reaction below the Coulomb barrier [26,27], and neutron capture [28]. Also previously inaccessible high spin states have now been discovered by γ spectroscopy with deep inelastic reactions [19,29,30]. The combined experimental information makes a detailed analysis possible, and the shell model is a well suited theoretical framework for this. The most basic and interesting point is to determine the interaction of the nucleons in the nucleus and to understand it.

ACKNOWLEDGMENT

We thank Jan Blomqvist, Stockholm, for very valuable hints and discussions.

APPENDIX A: EFFECTIVE $M1$- AND $E2$- MATRIX ELEMENTS AROUND ^{208}PB

Table V summarizes the reduced $M1$ and $E2$ matrix elements $\langle \mathrm{fin}\|M1\|\mathrm{init}\rangle$ and $\langle \mathrm{fin}\|E2\|\mathrm{init}\rangle$ that have been used in the analysis of the γ transitions in ^{208}Pb. Most values are from Donahue *et al.* [31], but a few signs have been corrected. For the hole states really the signs for holes are given, meaning that the signs of the $E2$ elements are the opposite of

those for particles. An interchange of initial and final state gives

$$\langle \text{fin}\|Op\|\text{init}\rangle = \langle \text{init}\|Op\|\text{fin}\rangle \times (-1)^{j_{\text{init}}-j_{\text{fin}}}.$$

Many values originate from the Migdal theory calculations of Ref. [34] for $M1$ and Ref. [36] for $E2$. These calculations include admixtures of the collective octupole excitation; this is appropriate for the present analysis, that also uses single particle orbitals which include such admixtures, not really pure orbitals. The calculations of the $M1$ elements have been proven to be correct in many instances. The calculated $\langle \pi h_{11/2}^{-1}\|M1\|\pi h_{11/2}^{-1}\rangle = 12.71$ nm agrees with the later measurement of 12.78(20) nm [37]. Likewise the calculation for $\langle \pi s_{1/2}^{-1}\|M1\|\pi s_{1/2}^{-1}\rangle = 2.32$ nm agrees with the experimental value 2.25(5) [33] and the theoretical $\langle \pi f_{7/2}\|M1\|\pi f_{7/2}\rangle = 8.41$ nm with 8.08(50) nm from experiment [35]. For the case of the $E2$ matrix elements the agreement is also quite good, the calculation of $\langle \pi i_{13/2}\|E2\|\pi i_{13/2}\rangle = -90.7$ e fm^2 and $\langle \nu i_{13/2}^{-1}\|E2\|\nu i_{13/2}^{-1}\rangle = 54.2$ e fm^2 correspond to experimental results of $-66(16)$ e fm^2 and 48.6(2) e fm^2, respectively.

[1] A. Heusler and P. von Brentano, Ann. Phys. (N.Y.) **75**, 381 (1973).

[2] William W. True, Chin W. Ma, and William T. Pinkston, Phys. Rev. C **3**, 2421 (1971).

[3] T. T. S. Kuo and G. H. Herling, Naval Research Laboratory Memorandum Report 2258, Washington, DC, 1971.

[4] T. T. S. Kuo and G. E. Brown, Nucl. Phys. **85**, 40 (1966).

[5] E. K. Warburton and B. A. Brown, Phys. Rev. C **43**, 602 (1991).

[6] M. Schramm, M. Rejmund, K. H. Maier, H. Grawe, and J. Blomqvist, Phys. Scr. **T56**, 307 (1995).

[7] K. H. Maier, Acta Phys. Pol. B **28**, 277 (1997).

[8] M. Schramm, Ph.D. thesis, Freie Universität Berlin, 1993, and Report of the Hahn-Meitner-Institut B-508 (1993), ISSN 0944-0305.

[9] M. Rejmund, Diploma thesis, Warsaw University, 1995.

[10] M. Schramm, K. H. Maier, M. Rejmund, L. D. Wood, N. Roy, A. Kuhnert, A. Aprahamian, J. Becker, M. Brinkman, D. J. Decman, E. A. Henry, R. Hoff, D. Manatt, L. G. Mann, R. A. Meyer, W. Stoeffl, G. Struble, and T.-F. Wang, Phys. Rev. C **56**, 1320 (1997).

[11] Minfang Yeh, dissertation, University of Kentucky, Lexington, Kentucky, 1997.

[12] Minfang Yeh, M. Kadi, P. E. Garrett, C. A. McGrath, S. W. Yates, and T. Belgya, Phys. Rev. C **57**, R2085 (1998).

[13] B. D. Valnion, dissertation an der Fakultät für Physik der Ludwig-Maximilians-Universität München, 1997.

[14] Aage Bohr and Ben R. Mottelson, *Nuclear Structure* (W. A. Benjamin, Inc., New York, 1969), formula 1A−72a, p. 84.

[15] E. K. Warburton (private communication).

[16] J. P. Bondorf, P. von Brentano, and P. Richard, Phys. Lett. **27B**, 5 (1968).

[17] Patrick Richard, P. von Brentano, H. Weiman, W. Wharton, W. G. Weitkamp, W. W. McDonald, and D. Spalding, Phys. Rev. **183**, 1007 (1996).

[18] N. Roy, K. H. Maier, A. Aprahamian, J. A. Becker, D. J. Decman, E. A. Henry, L. G. Mann, R. A. Meyer, W. Stöffl, and G. L. Struble, Phys. Lett. B **221**, 6 (1989).

[19] R. Broda, J. Wrzesinski, T. Pawlat, B. Fornal, Z. Grabowski, D. Bazzacco, S. Lunardi, C. Rossi-Alvarez, G. de Angelis, A. Gadea, and K. H. Maier, Proceedings of the Conference on Nuclear Structure at the Limits, Argonne, Illinois, 1996, ANL/Phy-97/1, p. 276.

[20] C. Fred Moore, J. G. Kulleck, Peter von Brentano, and and Frank Rickey, Phys. Rev. **164**, 1559 (1967).

[21] W. T. Wagner, G. M. Crawley, G. R. Hammerstein, and H. McManus, Phys. Rev. C **12**, 757 (1975).

[22] J. Lichtenstadt, C. N. Papanicolas, C. P. Sargent, J. Heisenberg, and J. S. McCarthy, Phys. Rev. Lett. **44**, 858 (1980).

[23] M. Moinester, J. P. Schiffer, and W. P. Alford, Phys. Rev. **179**, 984 (1969).

[24] J. P. Connelly, D. J. de Angelis, J. H. Heisenberg, F. W. Hersman, W. Kim, M. Leuschner, T. E. Millimann, J. Wise, and C. Papanicolas, Phys. Rev. C **45**, 2711 (1992).

[25] Ole Hansen, Nelson Stein, D. G. Burke, E. R. Flynn, J. D. Sherman, J. W. Sunier, and R. K. Sheline, Nucl. Phys. **A277**, 451 (1977).

[26] E. Radermacher, M. Wilhelm, S. Albers, J. Eberth, N. Nicolay, H. G. Thomas, H. Tiesler, P. von Brentano, R. Schwengner, S. Skoda, G. Winter, and K. H. Maier, Nucl. Phys. **A597**, 408 (1996).

[27] E. Radermacher, M. Wilhelm, P. von Brentano, and R. V. Jolos, Nucl. Phys. **A620**, 151 (1997).

[28] R. K. Sheline, R. L. Ponting, A. K. Jain, J. Kvasil, B. bu Nianga, and L. Nkwambiaya, Czech. J. Phys., Sect. B **39**, 22 (1989).

[29] M. Rejmund, K. H. Maier, R. Broda, M. Lach, J. Wrzesinski, J. Agramunt, J. Blomqvist, A. Gadea, J. Gerl, M. Gorska, H. Grawe, M. Kaspar, I. Kozhoukharov, I. Peter, H. Schaffner, R. Schubart, Ch. Schlegel, G. Stengel, S. Wan, and H. J. Wollersheim, Z. Phys. A **359**, 243 (1997).

[30] M. Rejmund, K. H. Maier, R. Broda, B. Fornal, M. Lach, J. Wrzesinski, J. Blomqvist, A. Gadea, J. Gerl, M. Gorska, H. Grawe, M. Kaspar, H. Schaffner, Ch. Schlegel, R. Schubart, and H. J. Wollersheim, Eur. Phys. J. A **1**, 261 (1998).

[31] D. J. Donahue, O. Häusser, R. L. Hershberger, R. L. Lutter, and F. Riess, Phys. Rev. C **12**, 1547 (1975).

[32] J. A. Becker, A. Berger, J. Blomqvist, D. J. Decman, R. Estep, E. Henry, K. H. Maier, L. G. Mann, R. A. Meyer, N. A. F. M. Poppelier, N. Roy, W. Stöffl, G. L. Struble, and L. D. Wood, Nucl. Phys. **A522**, 483 (1991).

[33] R. Neugart, H. H. Stroke, S. A. Ahmad, H. T. Duong, H. L. Ravn, and K. Wendt, Phys. Rev. Lett. **55**, 1559 (1985).

[34] R. Bauer, J. Speth, V. Klemt, P. Ring, E. Werner, and T. Yamazaki, Nucl. Phys. **A209**, 535 (1973).

[35] A. E. Stuchberry, A. P. Byrne, and G. D. Dracoulis, Nucl. Phys. **A555**, 369 (1993).

[36] P. Ring, R. Bauer, and J. Speth, Nucl. Phys. **A206**, 97 (1973).

[37] K. H. Maier, J. A. Becker, J. B. Carlson, R. G. Lanier, L. G. Mann, G. L. Struble, T. Nail, R. K. Sheline, W. Stöffl, and L. Ussery, Phys. Rev. Lett. **48**, 466 (1982).

[38] K. H. Maier, M. Menningen, L. E. Ussery, T. W. Nail, R. K. Sheline, J. A. Becker, D. J. Decman, R. G. Lanier, L. G. Mann, W. Stöffl, and G. L. Struble, Phys. Rev. C **30**, 1702 (1984),

recalibrated with the results of W. Tröger, T. Butz, P. Blaha, and K. Schwarz, Hyperfine Interact. **80**, 1109 (1993).

[39] D. J. Decman, J. A. Becker, J. B. Carlson, R. G. Lanier, L. G. Mann, G. L. Struble, K. H. Maier, W. Stöffl, R. K. Sheline, Phys. Rev. C **28**, 1060 (1983).

[40] Ch. Stenzel, H. Grawe, H. Haas, H.-E. Mahnke, and K. H. Maier, Nucl. Phys. **A411**, 248 (1983).

[41] H.-E. Mahnke, T. K. Alexander, H. R. Andrews, O. Häusser, P. Taras, D. Ward, E. Dafni, and G. D. Sprouse, Phys. Lett. **88B**, 48 (1979).

[42] Unknown value, but ≈ 0 because l forbidden.